Ketamine's rapid antidepressant effects are mediated by Ca^{2+}-permeable AMPA receptors in the hippocampus

Anastasiya Zaytseva[1,4], Evelina Bouckova[1,4], McKennon J. Wiles[1,4], Madison H. Wustrau[2,4], Isabella G. Schmidt[1,4], Hadassah Mendez-Vazquez[2], Latika Khatri[3], Seonil Kim[1,2*]

[1]Molecular, Cellular and Integrative Neurosciences Program,

[2]Department of Biomedical Sciences, Colorado State University, Fort Collin, CO 80523.

[3]Department of Cell Biology, New York University Grossman School of Medicine, New York, New York 10016.

[4]These authors contribute equally.

*Corresponding author: Seonil Kim

Email: seonil.kim@colostate.edu

This PDF file includes:

Main Text

Figures 1 to 7

Supplementary Figure 1

Abstract

Ketamine is shown to enhance excitatory synaptic drive in the hippocampus, which is presumed to underlie its rapid antidepressant effects. Moreover, ketamine's therapeutic actions are likely mediated by enhancing neuronal Ca^{2+} signaling. However, ketamine is a noncompetitive NMDA receptor (NMDAR) antagonist that inhibits excitatory synaptic transmission and postsynaptic Ca^{2+} signaling. Thus, it is a puzzling question how ketamine enhances glutamatergic and Ca^{2+} activity in neurons to induce rapid antidepressant effects while blocking NMDARs in the hippocampus. Here, we find that ketamine treatment for one hour in cultured mouse hippocampal neurons significantly reduces calcineurin activity to elevate AMPA receptor (AMPAR) subunit GluA1 phosphorylation. This phosphorylation ultimately induces the expression of Ca^{2+}-Permeable, GluA2-lacking, and GluA1-containing AMPARs (CP-AMPARs). Such ketamine-induced expression of CP-AMPARs enhances glutamatergic activity and synaptic plasticity in cultured hippocampal neurons. When a sub-anesthetic dose of ketamine is given to mice, it increases synaptic GluA1 levels, but not GluA2, and GluA1 phosphorylation in the hippocampus within one hour after treatment. These changes are likely mediated by ketamine-induced reduction of calcineurin activity in the hippocampus. Using the open field and tail suspension tests, we demonstrate that a low dose of ketamine rapidly reduces anxiety-like and depression-like behaviors in both male and female mice. However, when *in vivo* treatment of a CP-AMPAR antagonist abolishes the ketamine's effects on animals' behavior. We thus discover that ketamine at the low dose promotes the expression of CP-AMPARs via reduction of calcineurin activity in the hippocampus, which in turn enhances synaptic strength to induce rapid antidepressant actions.

Significance Statement

The main mechanisms believed to underlie ketamine's rapid antidepressant effects converge on enhancing glutamatergic activity and neuronal Ca^{2+}-dependent signaling in the brain. However, ketamine is an antagonist of NMDA receptors, major Ca^{2+} channels in excitatory synapses. Therefore, it is unclear how ketamine rapidly enhances glutamatergic activity and Ca^{2+} signaling. Our study fills this gap by discovering the molecular mechanisms of ketamine-induced Ca^{2+}-permeable AMPA receptor expression in the hippocampus within one hour after the treatment to produce antidepressant effects, which provides a better understanding of the mechanisms that contributes to enhancing synaptic plasticity and antidepressant behaviors following ketamine treatment.

Introduction

Major depressive disorder (MDD), also referred to as clinical depression, is a severe mood disorder with a large global prevalence (1). When depression co-occurs with chronic medical illnesses, untreated depression is linked to a lower quality of life, a higher risk of suicide, and impaired physical well-being (2-4). As such, it is understandable why MDD represents a serious public health concern. Many antidepressant drugs have been used by targeting the monoamine systems to increase the amount of serotonin or norepinephrine in the brain (5). However, it can take weeks or months for traditional antidepressants to fully manifest their therapeutic advantages (6). Moreover, less than 50% of all patients with depression have full remission with optimum treatment, thus there is still a great need for rapid medicinal relief to treat MDD (5).

Over the past 50 years, the use of ketamine for anesthesia has become widespread in both human and veterinary medicine (7). However, ketamine has also shown efficacy as a rapid-acting antidepressant only at low doses, particularly among those with treatment-resistant depression, while with increasing doses it evokes psychotomimetic actions and eventually produces anesthesia (8, 9). The main mechanism by which ketamine and other antidepressants produce their therapeutic benefits on mood recovery is the promotion of neuronal plasticity in the hippocampus (8, 10-12). However, ketamine is a noncompetitive NMDA receptor (NMDAR) antagonist that inhibits excitatory synaptic transmission (13). Therefore, by inhibiting glutamatergic NMDARs, ketamine can promote synaptic inhibition rather than excitation (14). Moreover, NMDARs are major Ca^{2+} channels in excitatory synapses (15). Ca^{2+} influx into the postsynaptic neurons through NMDARs activates multiple downstream pathways, contributing to depression and antidepressant actions (16). Therefore, ketamine-induced suppression of postsynaptic NMDARs deactivates Ca^{2+} signaling pathway. However, an

interesting aspects of ketamine's therapeutic actions are mediated by enhancing neuronal Ca^{2+} signaling (17, 18). Taken together, the main mechanisms believed to underlie ketamine's antidepressant effects converge on enhancing glutamatergic activity and neuronal Ca^{2+}-dependent signaling in the hippocampus (8, 11, 12, 16). Due to this, it becomes a puzzling question as to how ketamine rapidly enhances glutamatergic activity and Ca^{2+} signaling while blocking NMDARs in the hippocampus.

One prominent hypothesis to explain these paradoxical effects of ketamine is that it directly inhibits NMDARs on excitatory neurons, which induces a cell-autonomous form of homeostatic synaptic plasticity to increase excitatory synaptic activity onto these neurons (8, 11). This synaptic homeostasis is a negative-feedback response employed to compensate for functional disturbances in neurons and expressed via the regulation of glutamatergic AMPA receptor (AMPAR) trafficking and synaptic expression (19, 20). Postmortem studies have reported reductions in the mRNA expression levels of AMPAR subunit GluA1 and GluA3, but not GluA2, in the hippocampus of patients with depression (21), suggesting that subtype specific AMPAR decrease in the hippocampus is implicated in depression. Moreover, accumulating evidence supports the crucial involvement of AMPARs in mediating the antidepressant effects of ketamine (22-28). Interestingly, following ketamine treatment in animals, many studies find elevated levels of GluA1, particularly in the hippocampus, whereas the results of other subunits' expression are less consistent (23, 27-31). This suggests that subtype specific activation of AMPARs is crucial for ketamine's antidepressant actions. However, it is unknown how ketamine selectively affects AMPAR subtype-specific functions in the hippocampus.

There are two distinct types of AMPARs formed through combination of their subunits: Ca^{2+}-impermeable GluA2-containing AMPARs and Ca^{2+}-Permeable, GluA2-lacking, and GluA1-containing AMPARs (CP-AMPARs) (32, 33). Activity-dependent

AMPAR trafficking has long been known to be regulated by the phosphorylation of the GluA1 subunit (19). Phosphorylation of serine 845 (S845) in GluA1 promotes GluA1-containing AMPAR surface expression, whereas dephosphorylation of S845 is involved in receptor internalization (19, 34). We have previously shown that a decrease in neuronal Ca^{2+} activity reduces the activity of Ca^{2+}-dependent phosphatase calcineurin, increasing GluA1 S845 phosphorylation to induce synaptic expression of CP-AMPARs (35). It is thus possible that ketamine can reduce postsynaptic Ca^{2+} and calcineurin activity via NMDAR antagonism, which increases GluA1 S845 phosphorylation to induce CP-AMPAR expression and enhances glutamatergic synaptic transmission. Indeed, a prior study demonstrated that ketamine induces CP-AMPAR expression in spiny projection neurons in the nucleus accumbens, which is important for ketamine's antidepressant actions (36). However, it is uncertain whether GluA2-containing or GluA2-lacking AMPARs are inserted or removed from hippocampal synapses following ketamine administration. In the current study, using cultured mouse hippocampal neurons, we reveal that a one-hour treatment of low dose ketamine is sufficient to induce CP-AMPAR expression via reduction of calcineurin activity. Moreover, a low dose of ketamine in mice significantly reduces calcineurin activity and increases synaptic GluA1 levels, but not GluA2, in the hippocampus. Most importantly, ketamine at the low dose induces antidepression-like behaviors in mice within one hour after treatment, which is completely abolished by specifically blocking CP-AMPARs. Therefore, we discover a new molecular mechanism of ketamine's rapid antidepressant actions in which ketamine at the low doses promotes the expression of CP-AMPARs via reduction of calcineurin activity in the hippocampus within one hour after treatment, which in turn enhances synaptic strength to induce antidepressant effects.

Results

Ketamine treatment selectively increases GluA1-containing AMPAR surface expression by decreasing calcineurin activity in cultured mouse hippocampal neurons.

A large body of studies has found increased levels of GluA1 in the hippocampus after ketamine treatment in rodents, however the results for other subunits' expression are less reliable (23, 27-31). First, we examined whether ketamine treatment changed surface expression of AMPAR subunits in cultured mouse hippocampal neurons. We treated 14 days *in vitro* (DIV) cultured mouse hippocampal neurons with 1 μM ketamine, the estimated concentration in the human brain after intravenous infusion of the therapeutic dose (37), for one hour and measured surface expression of AMPAR subunit GluA1 and GluA2 using biotinylation and immunoblots as shown previously (35, 38-42). We found that ketamine treatment selectively increased surface expression of GluA1 when compared to the control (CTRL) (CTRL, 1.000 and ketamine, 1.598 ± 0.543, p = 0.002), but not GluA2 (CTRL, 1.000 and ketamine, 1.121 ± 0.464, p = 0.5195) (**Fig. 1a**). As GluA1 phosphorylation at serine 831 (pGluA1-S831) and serine 845 (pGluA1-S845) are known to regulate GluA1-containing AMPAR surface trafficking (19), we examined pGluA1-S831 and pGluA1-S845 levels one hour after 1 μM ketamine treatment in 14 DIV cultured hippocampal neurons as shown previously (34). We found significantly higher pGluA1-S831 (CTRL, 1.000 and ketamine, 1.967 ± 0.488, p = 0.0312) and pGluA1-S845 levels (CTRL, 1.000 and ketamine, 2.399 ± 1.024, p = 0.0312) in ketamine-treated neurons than in the control (CTRL) (**Fig. 1b**). This shows that ketamine treatment in cultured hippocampal neurons selectively increases GluA1 surface expression by increasing pGluA1-S831 and pGluA1-S845, which is consistent with the previous findings showing crucial role of GluA1 phosphorylation in rapid antidepressant

responses of ketamine (43-45).

We have previously shown that a decrease in Ca^{2+}-dependent phosphatase calcineurin activity significantly increases pGluA1-S845 and GluA1 surface expression (35). Previous studies have shown that 1 μM ketamine treatment can reduce ~ 50% of NMDA-induced currents (46), whereas 10 μM is sufficient to block ~ 80% of NMDA-induced currents (47). Therefore, ketamine treatment can reduce Ca^{2+} activity in neurons in the dosage-dependent manner, which in turn decreases calcineurin activity to elevate GluA1 phosphorylation and GluA1 surface expression. We thus examined whether ketamine treatment affected Ca^{2+} activity in 14 DIV cultured hippocampal excitatory neurons using the previously described method with modification (35, 38-42). For Ca^{2+} imaging, a genetically encoded Ca^{2+} indicator, GCaMP7s (48), was used to measure spontaneous somatic Ca^{2+} activity in cultured hippocampal excitatory neurons in the presence of 1, 10, or 20 μM ketamine. As consistent with the previous findings (46, 47), we found a significant reduction in Ca^{2+} activity in ketamine-treated neurons compared to control cells (CTRL) in the dosage-dependent manner (CTRL, 1.000 ± 0.432 $\Delta F/F_{min}$, 1 μM ketamine, 0.820 ± 0.363 $\Delta F/F_{min}$, $p = 0.036$, 10 μM ketamine, 0.069 ± 0.099 $\Delta F/F_{min}$, $p < 0.0001$, and 20 μM ketamine, 0.000 $\Delta F/F_{min}$, $p < 0.0001$) (**Fig. 1c**). This demonstrates that ketamine treatment significantly reduces neuronal Ca^{2+} activity in cultured hippocampal excitatory cells in the dosage-dependent manner.

To measure intracellular calcineurin activity directly, we used a Fluorescence Resonance Energy Transfer (FRET)-based calcineurin activity sensor as shown previously (35, 38, 39, 41, 49). We generated Sindbis virus to express the calcineurin activity sensor in cells (50). CFP, YFP, and FRET images in soma of 14 DIV cultured hippocampal neurons were acquired 36 hours after infection, and the emission ratio was calculated as shown previously (35, 38, 39, 41). We found that calcineurin activity was

significantly decreased after one-hour 1 μM ketamine treatment compared to the control (CTRL) (CTRL, 1.000 ± 0.106 and ketamine, 0.942 ± 0.051, $p = 0.0170$) (**Fig. 1d**). Following one hour treatment of 5 μM FK506, a calcineurin inhibitor (51), calcineurin activity was markedly reduced compared to the control (CTRL) (FK506, 0.806 ± 0.150, $p < 0.0001$) **(Fig. 1d**) as shown previously (35). Taken together, ketamine-mediated NMDAR antagonism reduces neuronal Ca^{2+} and calcineurin activity, which leads to a selective increase in GluA1 phosphorylation and GluA1-contraining AMPAR surface expression in cultured hippocampal neurons.

Ketamine treatment induces CP-AMPAR expression to enhance glutamatergic activity and synaptic plasticity in cultured mouse hippocampal neurons.

We next examined how ketamine affected glutamatergic activity in cultured hippocampal excitatory neurons. Given that neuronal Ca^{2+} is the secondary messenger responsible for transmitting depolarization status and synaptic activity (52), we carried out somatic Ca^{2+} imaging with glutamate uncaging in cultured mouse hippocampal excitatory neurons to measure glutamatergic activity. We treated 14 DIV hippocampal cultures with 1 μM ketamine for one hour and measured glutamate-induced Ca^{2+} signals. Glutamatergic activity was significantly higher in ketamine-treated neurons than control cells (CTRL) (CTRL, 1.000 ± 0.278 $\Delta F/F_0$ and ketamine, 1.289 ± 0.334 $\Delta F/F_0$, $p = 0.0022$) **(Fig. 2a**). CP-AMPARs have larger single channel conductance (19). Due to this, we examined whether an increase in glutamatergic activity following ketamine treatment was mediated by CP-AMPARs. To do so, we treated hippocampal neurons with 1 μM ketamine for one hour and carried out Ca^{2+} imaging with glutamate uncaging in the presence of 20 μM 1-naphthyl acetyl spermine (NASPM), a CP-AMPAR blocker. NASPM treatment was sufficient to abolish a ketamine-induced increase in

glutamatergic activity (Ketamine + NASPM, 0.961 ± 0.464 $\Delta F/F_0$, p = 0.0006), while it had no effect on control cells (CTRL) (CTRL + NASPM, 0.965 ± 0.350 $\Delta F/F_0$, p = 0.9603) (**Fig. 2a**). This shows that ketamine treatment induces CP-AMPAR expression and increases glutamatergic activity in cultured hippocampal excitatory neurons.

Ketamine's antidepressant effects are shown to be mediated by enhancing synaptic plasticity in the hippocampus, including long-term potentiation (LTP) (12, 53). Moreover, CP-AMPARs can initiate LTP in the hippocampus particularly when NMDARs are blocked (54). We thus treated 14 DIV cultured hippocampal neurons with a glycine-based media, well-established to induce a form of chemical LTP (cLTP) as shown previously (34, 40), to examine whether ketamine enhanced synaptic plasticity via the expression of CP-AMPARs. Following cLTP induction, pGluA1-S831 (CTRL, 1.000 and cLTP, 3.879 ± 1.764, p = 0.0027) and pGluA1-S845 levels (CTRL, 1.000 and cLTP, 4.658 ± 2.090, p = 0.0018) were significantly elevated in control neurons (CTRL), an indication of cLTP expression (**Fig. 2b-c**). We next treated neurons with 1 μM ketamine for one hour, then induced cLTP, and measured GluA1 phosphorylation. When compared to neurons without ketamine treatment, pGluA1-S831 (Ketamine + cLTP, 8.978 ± 4.861, p = 0.0276) and pGluA1-S845 levels (Ketamine + cLTP, 11.73 ± 6.717, p = 0.0311) were significantly higher in ketamine-treated neurons, an indication of enhanced cLTP expression (**Fig. 2b-c**). Importantly, a ketamine-induced increase in GluA1 phosphorylation was completely abolished when CP-AMPARs were blocked by treating neurons with 20 μM NASPM during cLTP (pGluA1-S831; Ketamine + cLTP + NASPM, 4.592 ± 3.343, p = 0.0299, and pGluA1-S845; Ketamine + cLTP + NASPM, 4.890 ± 3.301, p = 0.0279) (**Fig. 2b-c**). Notably, blocking CP-AMPARs had no effect on cLTP expression in the absence of ketamine treatment (pGluA1-S831; cLTP + NASPM, 3.684 ± 2.503, p = 0.7002, and pGluA1-S845; cLTP + NASPM, 3.724 ± 2.275, p =

0.4980) (**Fig. 2b-c**). Taken together, we demonstrate that ketamine enhances synaptic plasticity via the expression of CP-AMPARs in cultured hippocampal cells.

Synaptic GluA1 levels are selectively increased in the hippocampus following ketamine treatment.

Given that ketamine selectively increases GluA1 phosphorylation and GluA1-contraining AMPAR surface expression in cultured hippocampal neurons (**Fig. 1a-b**), we examined whether ketamine treatment upregulates synaptic GluA1 and GluA2 levels in the mouse hippocampus. A low dose of ketamine (10 mg/kg), a condition that is sufficient to change hippocampal AMPAR expression in mice (28), was intraperitoneally injected to 3-month-old male and female CD-1 mice, and saline was injected as a control. The postsynaptic density (PSD) fractions of the hippocampus were collected one hour after ketamine or saline injection, and synaptic GluA1, GluA2, pGluA1-S831, and pGluA1-S845 levels were measured by immunoblots as shown previously (38, 39, 55, 56). In male mice, we found GluA1 (CTRL, 1.000 and ketamine, 2.057 ± 0.763, p = 0.0005), pGluA1-S831 (CTRL, 1.000 and ketamine, 1.624 ± 0.489, p = 0.0158), and pGluA1-S845 levels (CTRL, 1.000 and ketamine, 1.480 ± 0.243, p = 0.0339), but not GluA2 levels (CTRL, 1.000 and ketamine, 1.088 ± 0.383, p > 0.9999), were significantly higher in the ketamine-treated hippocampal PSD fractions than the control (CTRL) (**Fig. 3a**). This shows that ketamine at the low dose significantly elevates synaptic GluA1 levels, which are likely mediated by increasing GluA1 phosphorylation in the male hippocampus, consistent with our findings in cultured hippocampal cells.

In contrast to male mice, 10 mg/kg ketamine injection in female mice significantly increased GluA1 (CTRL, 1.000 and ketamine, 1.224 ± 0.324, p = 0.0303), GluA2 (CTRL, 1.000 and ketamine, 1.393 ± 0.304, p = 0.0002), pGluA1-S831 (CTRL, 1.000 and

ketamine, 1.296 ± 0.319, $p = 0.0022$), and pGluA1-S845 levels (CTRL, 1.000 and ketamine, 1.394 ± 0.435, $p = 0.0014$) in the PSD fractions (**Fig. S1a**). This shows that ketamine at the low dose significantly increase both GluA1 and GluA2 levels in female hippocampal synapses. To address if this sex difference in ketamine's effects on synaptic AMPAR expression in the hippocampus is dependent on ketamine concentration, we used a lower dose of ketamine (5 mg/kg) in female mice and examined synaptic GluA1 and GluA2 expression in the hippocampus. The hippocampal PSD fractions were isolated one hour after 5 mg/kg ketamine or saline injection, and synaptic GluA1, GluA2, pGluA1-S831, and pGluA1-S845 levels were measured by immunoblots. Like male mice, synaptic GluA1 (CTRL, 1.000 and ketamine, 1.420 ± 0.361, $p = 0.0053$), pGluA1-S831 (CTRL, 1.000 and ketamine, 2.151 ± 1.337, $p = 0.0014$), and pGluA1-S845 levels (CTRL, 1.000 and ketamine, 2.330 ± 1.177, $p = 0.0031$) were significantly increased in the ketamine-treated female hippocampal synapses than the control, while GluA2 levels were not affected by ketamine (CTRL, 1.000 and ketamine, 0.952 ± 0.260, $p > 0.9999$) (**Fig. 3b**). This demonstrates that a lower dose of ketamine (5 mg/kg) is sufficient to increase synaptic GluA1 levels by increasing GluA1 phosphorylation in the female hippocampus.

Ketamine treatment significantly reduces anxiety-like behavior in mice, which requires CP-AMPARs.

We next examined whether ketamine treatment affects anxiety-like behavior in mice using the open field test as shown previously (57). 10 mg/kg ketamine was intraperitoneally injected to 3-month-old male and female CD-1 mice, and saline was administered to a control. One hour after the injection, we measured total distance traveled (locomotor activity) and total time spent outside and inside (anxiety-like

behavior) in the open field chamber. It has been shown that ketamine treatment in rodents induces hyperlocomotion and elevates time spent inside, an indication of reduced anxiety-like behavior (58-63). Consistent with these findings, ketamine injection significantly increased total distance travelled compared to controls (CTRL) in male mice, an indication of hyperlocomotion (CTRL, 34.244 ± 15.704 m and ketamine, 47.964 ± 0.361 m, $p = 0.0382$) (**Fig. 4a**). Furthermore, ketamine-treated male mice spent less time outside (CTRL, 1104.007 ± 54.881 seconds and ketamine, 1048.647 ± 50.779 seconds, $p = 0.0094$) but more time inside (CTRL, 95.993 ± 54.881 seconds and ketamine, 151.353 ± 50.779, $p = 0.0094$) than control mice, indicating decreased anxiety-like behavior (**Fig. 4a**). To determine whether CP-AMPARs were required for these behavioral changes, we intraperitoneally administered 10 mg/kg IEM-1460, the concentration that is sufficient to show drug effects in animals (64, 65), to ketamine-treated and saline-injected mice and performed the open field test one hour after drug injection. We found that blocking CP-AMPARs was sufficient to abolish the ketamine's effects in the open field test (Total distance travelled; Ketamine + IEM-1460, 33.069 ± 10.000 m, $p = 0.0129$, Time spent outside; Ketamine + IEM-1460, 1128.464 ± 27.927 seconds, $p = 0.0001$, and Time spent inside; Ketamine + IEM-1460, 71.536 ± 27.927 seconds, $p = 0.0001$) (**Fig. 4a**). Conversely, IEM-1460 treatment had no effect on animals' behavior in the absence of ketamine (Total distance travelled; CTRL + IEM-1460, 30.782 ± 13.867 m, $p = 0.8087$, Time spent outside; CTRL + IEM-1460, 1134.809 ± 44.172 seconds, $p = 0.3410$, and Time spent inside; CTRL + IEM-1460, 65.191 ± 44.172 seconds, $p = 0.3410$) (**Fig. 4a**). This shows that 10 mg/kg ketamine treatment significantly reduces male animals' anxiety-like behavior in the open field test, which is mediated by CP-AMPARs.

In female mice, unlike male animals, 10 mg/kg ketamine had no effect on

locomotor activity (CTRL, 42.287 ± 10.576 m and ketamine, 40.848 ± 11.091 m, p = 0.9804) (**Fig. S1b**). However, like male mice, 10 mg/kg ketamine significantly reduced time spent outside (CTRL, 1103.561 ± 24.289 seconds and ketamine, 1062.840 ± 54.145 seconds, p = 0.0330) but increased time spent inside (CTRL, 96.439 ± 24.289 seconds and ketamine, 137.160 ± 54.145, p = 0.0330), an indication of reduced anxiety-like behavior (**Fig. S1b**). To examine the role of CP-AMPARs in these behavioral changes, we intraperitoneally administered 10 mg/kg IEM-1460 and performed the open field test one hour after drug injection as described above. IEM-1460 injection had no effect on locomotor activity (Total distance travelled; CTRL + IEM-1460, 37.971 ± 13.870m, p = 0.7456 and Ketamine + IEM-1460, 37.576 ± 11.093 m, p = 0.8239) (**Fig. S1b**). However, *in vivo* CP-AMPAR inhibition was sufficient to reverse ketamine-induced behavioral changes (Time spent outside; Ketamine + IEM-1460, 1116.100 ± 44.791 seconds, p = 0.0033, and Time spent inside; Ketamine + IEM-1460, 83.900 ± 44.791 seconds, p = 0.0033) (**Fig. S1b**). Like male mice, IEM-1460 treatment had no effect on behaviors in the open field test in the absence of ketamine (Total distance travelled; CTRL + IEM-1460, 37.971 ± 13.870 m, p = 0.7456, Time spent outside; CTRL + IEM-1460, 1119.917 ± 50.469 seconds, p = 0.7602, and Time spent inside; CTRL + IEM-1460, 80.083 ± 50.469 seconds, p = 0.7602) (**Fig. S1b**). Given that a lower dose of ketamine (5 mg/kg) selectively increases synaptic GluA1 levels, but not GluA2, in the female hippocampus (**Fig. 3b**), we intraperitoneally injected 5 mg/kg ketamine to 3-month-old female CD-1 mice and carried out the open field test as stated above. 5 mg/kg ketamine treatment in female mice was unable to increase locomotor activity (CTRL, 42.648 ± 10.103 m and ketamine, 44.736 ± 8.647 m, p = 0.9751), but CP-AMPAR inhibition significantly reduced locomotion only in ketamine-treated female mice (CTRL + IEM-1460, 40.098 ± 12.326 m, p = 0.9408, and ketamine + IEM-1460, 25.605 ±

16.439 m, p = 0.0080) **(Fig. 4b**). This indicates that a lower dose of ketamine induces the expression of CP-AMPARs, contributing to locomotor activity in female mice. In addition, like 10 mg/kg ketamine treatment in male and female mice, 5 mg/kg ketamine injection in female animals significantly reduced anxiety-like behavior (Time spent outside; CTRL, 1096.190 ± 32.931 seconds, and Ketamine, 1011.288 ± 66.949 seconds, p = 0.0029, and Time spent inside; CTRL, 103.810 ± 32.931 seconds, and Ketamine, 188.713 ± 66.949 seconds, p = 0.0029), which was mediated by CP-AMPARs (Time spent outside; CTRL + IEM-1460, 1114.636 ± 49.333 seconds, p = 0.8026, and Ketamine + IEM-1460, 1121.520 ± 79.288 seconds, p = 0.0005, and Time spent inside; CTRL + IEM-1460, 85.364 ± 49.333 seconds, p = 0.8026, and Ketamine + IEM-1460, 78.480 ± 79.288 seconds, p = 0.0005) (**Fig. 4b**). This indicates that 10 mg/kg and 5 mg/kg ketamine treatment in female mice significantly decrease anxiety-like behavior in the open field test, which is dependent on CP-AMPARs.

Ketamine treatment significantly reduces depression-like behavior in mice, which requires CP-AMPARs.

We next used a tail suspension test as shown previously (56) to address whether ketamine-induced antidepressant actions were dependent on CP-AMPARs. 10 mg/kg ketamine was intraperitoneally injected to male and female 3-month-old CD-1 mice, and saline was administered to a control. As immobility in the tail suspension test is correlated with the depression-like state of the animals (56), we measured immobility and found that ketamine injection in male mice significantly decreased immobility relative to the control (CTRL) (CTRL, 198.183 ± 32.632 seconds and ketamine, 153.569 ± 54.145 seconds, p = 0.0164), an indication of reduced depression-like behavior (**Fig. 5a**). IEM-1460 treatment was sufficient to reverse ketamine-induced antidepressant

effects on the tail suspension test (Ketamine + IEM-1460, 195.100 ± 47.681 seconds, $p = 0.0285$), while it had no effect on immobility in control animals (CTRL) (CTRL + IEM-1460, 206.578 ± 31.598 seconds, $p = 0.9504$) (**Fig. 5a**). This demonstrates that 10 mg/kg ketamine treatment in male mice significantly reduces depression-like behavior, which is mediated by CP-AMPARs.

Unlike male animals, 10 mg/kg ketamine injection to female mice showed no antidepressant effects on our tail suspension test (CTRL, 170.550 ± 48.708 seconds and ketamine, 192.433 ± 50.495 seconds, $p = 0.7826$) (**Fig. S1c**). Moreover, IEM-1460 treatment was unable to affect depression-like behavior in female mice (CTRL + IEM-1460, 178.775 ± 55.421 seconds, $p = 0.9885$, and ketamine + IEM-1460, 183.517 ± 61.042 seconds, $p = 0.9776$) (**Fig. S1c**). We thus treat 3-month-old female CD-1 mice with 5 mg/kg ketamine as described above and performed the tail suspension test. A lower dose of ketamine in female mice significantly decreased immobility in the tail suspension test (CTRL, 212.760 ± 37.207 seconds and ketamine, 130.273 ± 52.945 seconds, $p = 0.0026$) (**Fig. 5b**). Most importantly, CP-AMPAR antagonist treatment prevented ketamine's antidepressant effect (Ketamine + IEM-1460, 203.170 ± 64.843 seconds, $p = 0.0087$), while it had no effect on immobility in control animals (CTRL + IEM-1460, 214.050 ± 28.469 seconds, $p > 0.9999$) (**Fig. 5b**). This shows that a lower dose of ketamine (5 mg/kg) is sufficient to induce antidepressant effects in female mice, which requires CP-AMPARs, like male animals.

Ketamine treatment significantly reduces calcineurin activity in the hippocampus.

Ketamine injection selectively increased synaptic GluA1 expression and its phosphorylation in the male and female hippocampus (**Fig. 3a-b**). We also revealed that CP-AMPARs were required for ketamine-induced antidepressant actions in male and

female mice **(Fig. 4 and 5**). Given our *in vitro* experiments showed that a ketamine-induced decrease in calcineurin activity played crucial roles in GluA1-containing AMPAR surface expression (**Fig. 1c-d**), we virally expressed the FRET-based calcineurin activity sensor in the hippocampus to determine whether ketamine reduced calcineurin activity. To express the calcineurin activity sensor, Sindbis virus was stereotaxically injected into the hippocampal CA1 area of 3-month-old male and female CD-1 mice. Ketamine was intraperitoneally injected to animals 36 hours after the infection to ensure viral calcineurin activity sensor expression, and saline was administered as the control (CTRL). CFP, YFP, and FRET images were acquired in soma of CA1 pyramidal neurons, and the emission ratio was calculated as shown in **Fig. 1d**. We found that calcineurin activity in the male hippocampus was significantly decreased after one-hour 10 mg/kg ketamine treatment compared to the saline-treated hippocampus (CTRL) (CTRL, 1.000 ± 0.382 and ketamine, 0.846 ± 0.313, $p = 0.0164$) (**Fig. 6a**). We also injected 5 mg/kg ketamine to female mice and measured calcineurin activity in hippocampal CA1 neurons. Like the male hippocampus, one-hour 5 mg/kg ketamine treatment significantly reduced calcineurin activity in the female hippocampus (CTRL, 1.000 ± 0.419 and ketamine, 0.812 ± 0.338, $p = 0.0011$) (**Fig. 6b**). Therefore, ketamine treatment significantly reduces calcineurin activity in the hippocampus, which likely leads to an increase in GluA1 phosphorylation and the expression of CP-AMPARs. These glutamatergic changes in the hippocampus contribute to ketamine-induced antidepressant actions in animals.

Discussion

Although an elevation of glutamatergic activity and neuronal Ca^{2+}-dependent signaling in the brain is thought to induce ketamine's antidepressant effects (8, 11, 12, 16), it is unclear how ketamine enhances these activities due to its nature of NMDAR antagonism. It has been suggested that ketamine's antidepressant effects are initiated by directly targeting NMDARs on excitatory neurons through a cell intrinsic mechanism (8). Ketamine can disrupt NMDAR basal activation on excitatory neurons. When this activity is reduced, a mechanism of homeostatic synaptic plasticity is activated, which causes a rapid increase in excitatory synaptic responses in these neurons as a form of compensation (8). We and others have previously found that neuronal activity deprivation-induced homeostatic synaptic up-scaling can elevate glutamatergic synaptic activity and Ca^{2+}-dependent signaling via the expression of CP-AMPARs (35, 66, 67). CP-AMPARs could thus be an ideal candidate to counteract ketamine-induced NMDAR inhibition in synaptic plasticity and neuronal Ca^{2+} signaling. In fact, studies in preclinical animal models have further demonstrated the necessity of AMPARs for the effects of ketamine, however their precise function is yet unknown (8). Here, our new findings demonstrate how ketamine rapidly induces CP-AMPAR expression in hippocampal excitatory neurons to adjust synaptic activity in the control of antidepressant behaviors.

Although a large group of AMPAR auxiliary subunits can provide heterogeneity of AMPAR trafficking (68), activity-dependent receptor trafficking has long been known to be regulated by the phosphorylation of GluA1 mainly in a two-step process (19, 69). First, GluA1 S845 phosphorylation is mediated by cAMP-dependent protein kinase A (PKA) or cGMP-dependent protein kinase II (cGKII) (70-72). Importantly, GluA1 S845 phosphorylation promotes GluA1 surface expression and mediates LTP (19, 35, 38, 73-80). In contrast, calcineurin-mediated dephosphorylation of GluA1 S845 is involved in

receptor internalization (19, 35, 38, 73-80). Second, when GluA1 is additionally phosphorylated at S831 by Ca^{2+}/calmodulin-dependent protein kinase II (CaMKII) or protein kinase C (PKC), and GluA1-containing AMPARs are targeted to the PSD, contributing to the enhanced synaptic transmission following LTP induction (69, 73, 80-83). Therefore, cooperative phosphorylation on GluA1 plays important roles in AMPAR trafficking and function in excitatory synapses (**Fig. 7a**). Our new data suggest that ketamine-induced NMDAR antagonism significantly decreases neuronal Ca^{2+} activity and subsequently calcineurin activity, leading to an increase in GluA1-containing, GluA2-lacking CP-AMPAR expression in the hippocampus via the elevation of GluA1 phosphorylation within one hour after ketamine treatment. Previous studies also demonstrate data consistent with our findings that GluA1 phosphorylation is crucial for ketamine-induced antidepressant effects in animals (43-45). These changes in glutamatergic synapses enhances synaptic plasticity in the hippocampus, which contributes to antidepressant effects in animals (**Fig. 7b**). Taken together, we discover the molecular mechanisms of the ketamine-induced CP-AMPAR expression in the hippocampus, which provides a better insight into the mechanisms that contributes to changes in synaptic plasticity and behaviors following ketamine treatment.

Although we and others show that GluA1 levels are selectively increased in the hippocampus within one hour after ketamine treatment in mice (23, 27-31), other groups have also demonstrated an increase in both GluA1 and GluA2 levels following ketamine treatment (27, 28). Interestingly, GluA1 and GluA2 levels were measured more than one hour after ketamine treatment in these studies. It has been suggested that the insertion of CP-AMPARs in hippocampal synapses is only transient (less than one hour) following LTP induction (84). Then, they are replaced by Ca^{2+}-Impermeable, GluA2-containing AMPARs (CI-AMPARs) because CP-AMPARs likely induce neurotoxicity via sustained

synaptic Ca^{2+} entry (84-86). The discrepancy between our findings and those of others may therefore be due to the differences within ketamine treatment incubation time. In addition, other studies show no change in GluA1 and GluA2 levels after ketamine treatment (87, 88). Notably, these studies examine ketamine effects in the frontal cortex or the mesolimbic circuit. Therefore, it is possible that ketamine may differentially affect glutamatergic synapses in different brain regions.

One significant discovery of our study is that, in contrast to male animals, female mice express CP-AMPARs after receiving a lower dose of ketamine, which promotes the antidepressant effects, an indication of enhanced ketamine antidepressant responses in female animals. In fact, several studies using both male and female animals show an increased sensitivity to ketamine in females. Stress-naïve female rodents consistently respond to a lower dose of ketamine than male animals on depression-like behavioral tests, including forced swim test and novelty suppressed feeding test (28, 89-91). One possible explanation of enhanced ketamine antidepressant responses in female rodents is different pharmacokinetics of ketamine in plasma and brain of the animals (92). When compared to male rats, in female animals, higher concentrations of ketamine and norketamine, a ketamine's metabolite, are found in the medial prefrontal cortex and hippocampus over the 3-hour time course following treatment (92). The study further demonstrates that longer half-lives and slower clearance rates in female rats contribute to greater effects of ketamine and its metabolites after treatment (92). In addition, sex differences in the antidepressant activity of ketamine have shown to be mediated by sex hormones (90). Indeed, previous studies have been able to demonstrate a crucial role for ovarian hormones in the increased female behavioral sensitivity to low-dose ketamine (90, 93). However, proestrus and diestrus female rats show no significant different pharmacokinetic profiles of ketamine, suggesting that sexual hormones have a

stronger effect on ketamine downstream signaling pathways than the pharmacokinetic systems when it comes to causing sex-dependent behavioral sensitivity to ketamine (92). Interestingly, ketamine and its two active metabolites, (*2R,6R*)-hydroxynorketamine (HNK) and (*2S,6S*)-HNK, can directly bind to estrogen receptor alpha (ERα) to increase GluA1 and GluA2 levels, an indication of AMPAR activation, which plays a key role in ketamine's antidepressant effects (94). Moreover, estradiol, the most potent and prevalent estrogen, is known to upregulate AMPAR functions by an increase in surface GluA2 levels (95, 96). This is consistent with our findings in which both GluA1 and GluA2 expression is significantly increased in the female hippocampus when 10 mg/kg ketamine is injected (**Fig. S1a**). Given that IEM-1460 treatment reverses anxiolytic behavior in female mice treated with 10 mg/kg ketamine (**Fig. S1b**), this dose of ketamine induces the expression of both CP-AMPARs and CI-AMPARs in the female hippocampus. Importantly, more women than men are diagnosed with depression (97-99), which has been explained by the sex differences in the brain's structure and function as well as by the presence of sexually dimorphic hormones (100, 101). However, the potential sex differences in response to ketamine have been particularly understudied at this time. Therefore, further discussion of the sex differences in the antidepressant activity of ketamine is needed.

A common etiological element in the production of major depression in humans is exposure to significant and frequently chronic psychological stress or trauma (102, 103). However, the results from studies in a variety of mice strains generally show that ketamine has similar antidepressant effects in naïve animals rather than having opposing effects in the presence or absence of chronic stress (104), consistent with our current findings. Nonetheless, there are mixed reports on ketamine's effects in naïve controls (89, 105-108). Moreover, a recent clinical study reveals that a single infusion of

ketamine shows therapeutic effects in patients with treatment-resistant depression, while it induces depressive symptoms in healthy individuals (109). This indicates the importance of stressed states in determining the brain response to ketamine. Therefore, valid animal models of ketamine-induced antidepressant treatment will benefit by exhibiting stress-dependent behavioral responses.

Here, we demonstrate that the mechanisms of CP-AMPAR-dependent homeostatic synaptic plasticity mediates ketamine's antidepressant effects, which is based on NMDAR antagonism. Another hypothesis to explain ketamine's antidepressant effects is that ketamine acts by directly inhibiting NMDARs localized on inhibitory interneurons, causing disinhibition of glutamatergic neurons and a resultant rapid increase in excitatory synaptic transmission in the prefrontal cortex (17, 110). However, it is not completely understood how ketamine selectively inhibits NMDARs on inhibitory cells, given that the receptors are expressed in other cell types, including excitatory neurons. Although many previous studies aiming to understand the ketamine effects have largely focused on NMDAR inhibition (7), contradictory results have been reported describing the NMDAR inhibition-dependent mechanisms (17, 28, 110, 111). Moreover, the results of many human treatment trials indicate that other NMDAR antagonists lack the antidepressant properties of ketamine (112) although the United States Food and Drug Administration (FDA) recently approved one NMDAR antagonist for MDD. This suggests that ketamine's therapeutic actions likely involve additional mechanisms, including synaptic plasticity strengthening, AMPAR activation, synaptogenesis, enhanced brain-derived neurotrophic factor (BDNF) signaling, and activation of mammalian target of rapamycin (mTOR) (111). In-depth investigations into the precise mechanisms underlying ketamine's effects have significantly advanced our understanding of depression and sparked the development of new ideas in molecular

and cellular neuropharmacology. However, many basic and clinical questions regarding ketamine's antidepressant effects remain unanswered (7). Therefore, future research will be needed to increase our comprehension of the pharmacological and neurobiological mechanisms of ketamine in the treatment of psychiatric diseases by addressing these questions.

Materials and Methods

Animals

CD-1 mice were obtained from Charles River and bred in the animal facility at Colorado State University (CSU). Animals were housed under 12:12 hour light/dark cycle. 3-month-old male and female CD-1 mice were used in the current study. CSU's Institutional Animal Care and Use Committee (IACUC) reviewed and approved the animal care and protocol (3408).

Primary hippocampal neuronal culture

Postnatal day 0 (P0) male and female CD-1 pups were used to produce mouse hippocampal neuron cultures as shown previously (34, 42, 113). Hippocampi were isolated from P0 CD-1 mouse brain tissues and digested with 10 U/mL papain (Worthington Biochemical Corp. Lakewood, NJ). Mouse hippocampal neurons were plated on following poly lysine-coated dishes for each experiment - glass bottom dishes (500,000 cells) for Ca^{2+} imaging and FRET analysis, and 6 cm dishes (2,000,000 cells) for biochemical experiments. Cells were grown in Neurobasal Medium (Thermo Fisher Scientific) with B27 supplement (Thermo Fisher Scientific), 0.5 mM Glutamax (Thermo Fisher Scientific), and 1% penicillin/streptomycin (Thermo Fisher Scientific).

Reagents

Ketamine hydrochloride (VetOne) was used in both *in vitro* and *in vivo* experiments. For neuronal cultures, we used 1, 10, or 20 μM ketamine. For mice, 5 mg/kg or 10 mg/kg ketamine was intraperitoneally injected to 3-month-old male and female CD-1 mice. We have an approval from IACUC to use ketamine and have the United States Drug Enforcement Administration license to use ketamine for research

purpose (DEA# RK0573863). 1.2 g/kg urethane (Sigma) was used for anesthetizing mice for stereotaxic surgery. 5 μM FK506 (Tocris) was used to inhibit calcineurin activity in cultured hippocampal excitatory neurons. 2 μM tetrodotoxin (TTX) (Abcam) was used to block spontaneous Ca^{2+} activity in cultured hippocampal excitatory neurons. 1 μM 4-methoxy-7-nitroindolinyl (MNI)-caged L-glutamate (Tocris) was added to the culture media for glutamate uncaging. 20 μM 1-naphthyl acetyl spermine (NASPM, Abcam) was used to block CP-AMPARs in cultured hippocampal excitatory neurons. 10 mg/kg IEM-1460 (Tocris) was intraperitoneally injected to 3-month-old male and female CD-1 mice to inhibit *in vivo* CP-AMPAR activity because it is blood-brain barrier (BBB)-permeable (64, 65, 114).

Surface Biotinylation

Surface biotinylation was performed according to the previous studies (35, 38-42). Cells were washed with ice-cold PBS containing 1 mM $CaCl_2$ and 0.5 mM $MgCl_2$ and incubated with 1 mg/ml Sulfo-NHS-SS-biotin (Thermo Fisher Scientific) for 15 minutes on ice. Following biotin incubation, neurons were washed with 20 mM glycine to remove the excess of biotin, and cells were lysed in 300 μl RIPA buffer for one hour. 10% of total protein was separated as input samples, and protein lysates were incubated overnight with streptavidin-coated beads (Thermo Fisher Scientific) at 4°C under constant rocking. The beads containing surface biotinylated proteins were separated by centrifugation. Biotinylated proteins were eluted from streptavidin beads with SDS loading buffer. Surface protein fractions and their corresponding total protein samples were analyzed by immunoblots.

Chemical LTP (cLTP)

cLTP protocol was followed as previously described (34, 40, 79). 14 DIV hippocampal cultured neurons were washed 3 times in Mg^{2+} free buffer (150 mM NaCl, 2 mM $CaCl_2$, 5 mM KCl, 10 mM HEPES, 30 mM glucose, 1 μM strychnine (Tocris), and 20 μM bicuculline (Abcam) and incubated in glycine buffer (Mg^{2+} free buffer with 0.2 mM glycine) at 37°C for 5 minutes. Then, Mg^{2+} buffer (Mg^{2+} free buffer with 2 mM $MgCl_2$) was added to block NMDARs and cells were incubated at 37°C for 30 minutes before being processed for immunoblots. To inhibit CP-AMPARs, we added 20 μM NASPM in Mg^{2+} buffer.

Immunoblots

Immunoblots were performed as described previously (34, 35, 38-42, 55-57, 113, 115-118). The protein concentration in total cell lysates was determined by a BCA protein assay kit (Thermo Fisher Scientific). Equal amounts of protein samples were loaded on 10% glycine-SDS-PAGE gel. The gels were transferred to nitrocellulose membranes. The membranes were blocked (5% powdered milk) for 1 hour at room temperature, followed by overnight incubation with the primary antibodies at 4°C. The primary antibodies consisted of anti-GluA1 (Millipore, 1:2000), anti-GluA2 (Abcam, 1:2000), anti-phosphorylated GluA1-S831 (Millipore, 1:1000), anti-phosphorylated GluA1-S845 (Millipore, 1:1000), and anti-actin (Abcam, 1:2000) antibodies. Membranes were subsequently incubated by secondary antibodies for 1 hour at room temperature and developed with Enhanced Chemiluminescence (ECL) (Thermo Fisher Scientific, Waltham, MA). Protein bands were quantified using ImageJ (https://imagej.nih.gov/ij/).

GCaMP Ca^{2+} Imaging

To measure Ca^{2+} activity in cultured hippocampal excitatory neurons, we infected

4 DIV neurons with adeno-associated virus (AAV) expressing CamK2a-Cre (Addgene# 105558-AAV1) - pENN.AAV.CamKII 0.4.Cre.SV40 was a gift from James M. Wilson (Addgene plasmid # 105558 ; http://n2t.net/addgene:105558 ; RRID:Addgene_105558) - and Cre-dependent GCaMP7s (Addgene# 104495-AAV1) - pGP-AAV-CAG-FLEX-jGCaMP7s-WPRE was a gift from Douglas Kim & GENIE Project (Addgene plasmid # 104495 ; http://n2t.net/addgene:104495 ; RRID:Addgene_104495) - (48) because when AAVs of the same serotype are co-infected, many neurons are transduced by both viruses (119). Neurons were grown in Neurobasal Medium without phenol red (Thermo Fisher Scientific) and with B27 supplement (Thermo Fisher Scientific), 0.5 mM Glutamax (Thermo Fisher Scientific), and 1% penicillin/streptomycin (Thermo Fisher Scientific). We then measured Ca^{2+} activity in 14 DIV cultured hippocampal excitatory neurons with a modification of the previously described method (35, 38-42). Glass-bottom dishes were mounted on a temperature-controlled stage on an Olympus IX73 microscope and maintained at 37°C and 5% CO_2 using a Tokai-Hit heating stage and digital temperature and humidity controller. For GCaMP7s, the images were captured right after 1, 10, or 20 μM ketamine was added to the media with a 10 ms exposure time and a total of 100 images were obtained with a one-second interval. F_{min} was determined as the minimum fluorescence value during the imaging. Total Ca^{2+} activity was obtained by 100 values of $\Delta F/F_{min} = (F_t - F_{min}) / F_{min}$ in each image, and values of $\Delta F/F_{min} < 0.1$ were rejected due to potential photobleaching. The average total Ca^{2+} activity in the control group was used to normalize total Ca^{2+} activity in each cell. The control group's average total Ca^{2+} activity was compared to the experimental groups' average as described previously (35, 38-42).

GCaMP Ca^{2+} Imaging with glutamate uncaging

We carried out Ca^{2+} imaging with glutamate uncaging as shown previously (120) in cultured hippocampal neurons one hour after 1 μM ketamine treatment. In addition, we added 20 μM NASPM right before Ca^{2+} imaging to inhibit CP-AMPARs. For glutamate uncaging, 1 μM 4-methoxy-7-nitroindolinyl (MNI)-caged L-glutamate was added to the culture media, and epi-illumination photolysis (390 nm, 0.12 mW/mm^2, 1 ms) was used. 2 μM TTX was added to prevent action potential-dependent network activity. A baseline average of 20 frames (50 ms exposure) (F_0) were captured prior to glutamate uncaging, and 50 more frames (50 ms exposure) were obtained after single photostimulation. The fractional change in fluorescence intensity relative to baseline ($\Delta F/F_0$) was calculated. The average peak amplitude in the control group was used to normalize the peak amplitude in each cell. The control group's average peak amplitude was compared to the experimental groups' average.

Sindbis virus infection in cultured neurons

Sindbis virus expressing the calcineurin activity sensor was produced as described previously (50). Calcineurin activity sensor cDNA (CaNAR) (a gift from Jin Zhang at Johns Hopkins University) was subcloned into pSinRep5 vector. BHK cells were electroporated with RNA of pSinRep5–CaNAR according to Sindbis Expression System manual (Invitrogen). The pseudovirions-containing medium was collected 24 hours after electroporation, and the titer for the construct was tested empirically in neuronal cultures. To express the calcineurin activity sensor in cultured neurons, 14 DIV neurons were infected with a titer resulting in infection of 20% of neurons (typically 1 μl of α-MEM virus stock diluted in 600 μl conditioned neurobasal-B27 medium per glass-bottom dish). It has been shown previously that no apparent adverse effects on morphology of the infected neurons was observed for up to 3 days postinfection (50).

Cells were treated with 1 μM ketamine and/or 20 μM NASPM or 5 μM FK506 for one hour 24 hours after infection and fixed to analyze calcineurin activity.

Sindbis virus infection in the mouse hippocampus

We virally expressed the calcineurin activity sensor using bilateral stereotaxic injection in the mouse hippocampus. Animals (3-month-old male and female CD-1 mice) were anaesthetized with 1.2 g/kg urethane. Anesthetic depth was confirmed with pedal response (foot retraction, response to non-damaging pressure of footpads using tweezers), ear twitch responses, and respiratory rates. Animal temperature was maintained with heating pads or warming gel packs. Once it was confirmed that the mice were properly anesthetized, the surgical field of the head of mice was aseptically prepared (shaved and prepped with betadine and alcohol). Animals were then placed in a stereotaxic frame (Stoelting). A small incision of the scalp was made with a sterile #10 surgical blade. With the aid of stereotaxic mounting equipment, a small hole was drilled in the bone using a high-speed drill and a dental bone drill bit, which has been sterilized. When the dura was exposed, a small pin hole was made, and a sterile syringe to inject Sindbis virus expressing the calcineurin activity sensor (1 μl) was lowered to the hippocampal CA1 area (Bregma coordinates: AP: − 1.95 mm, ML: ± 1.12 mm, DV: − 1.20 mm). During surgery, anesthetic depth was monitored every 5 minutes using pedal responses and respiration rates. After surgery, animals were allowed to recover from the anesthesia before being returned to their cages, and their health was closely monitored. Mice received analgesic doses of buprenorphine every 12 hours for one day after surgery. Buprenorphine was delivered by subcutaneous injection (0.1 mg/kg). Mice were monitored for any of the following signs of prolonged discomfort and pain: aggressiveness, hunched posture, failure to groom, awkward gait, vocalization,

greater or less tissue coloration, eye discoloration, abnormal activity (usually less), hesitancy to move (especially in response to startle), water consumption, or food intake. Because neurons in the brains are preferentially infected with Sindbis virus at 36 hours after infection (121), 10 mg/kg ketamine and/or 10 mg/kg IEM-1460 was intraperitoneally injected to animals 36 hours after the infection to ensure viral calcineurin activity sensor expression, and saline was administered to controls. Brain tissues were isolated one hour after treatment, fixed, and sectioned at 40 μm by using a vibratome. Hippocampal sections in each mouse were used imaged for hippocampal calcineurin activity.

FRET analysis

Calcineurin activity was determined by the FRET emission ratio as described previously (35). CFP, YFP, and FRET images were acquired in the soma, and the following formula was used to calculate the emission ratio: *(FRET channel emission intensity – FRET channel emission intensity of background) / (CFP channel emission intensity – CFP channel emission intensity of background)* as described previously (35, 39, 41). The higher emission ratio indicates the higher calcineurin activity.

Behavioral tests

We measured locomotor activity and anxiety-like behavior using the open field test as carried out previously (57). The test mouse was first placed in the center of the open field chamber (40 W x 40 L x 40 H cm) for 5 minutes. Animals were then allowed to explore the chamber for 20 minutes. A 20 x 20 cm center square was defined as the inside zone. The tail suspension test was performed as described previously (56). The

test mouse was suspended by its tails from a rod suspended 20 cm above the tabletop surface with adhesive tape placed 1 cm from the tip of the tail. Animals were immobile when they exhibited no body movement and hung passively for > 3 seconds. The time during which mice remained immobile was quantified over a period of 6 minutes. Mice that successfully climbed their tails to escape were excluded from the analysis. The behavior was recorded by a video camera. Data were analyzed using the ANY-maze tracking program to acquire total traveled distance (locomotor activity) and time spent outside and inside (anxiety-like behavior) for the open field test and immobility (depression-like behavior) for the tail suspension test. All behavior tests were blindly scored by more than two investigators.

Statistical analysis

The Franklin A. Graybill Statistical Laboratory at CSU has been consulted for statistical analysis in the current study, including experiment conception and design, data analysis, and interpretation. We used the GraphPad Prism 9 software to determine statistical significance (set at $p < 0.05$). Grouped results of single comparisons were tested for normality with the Shapiro-Wilk normality or Kolmogorov-Smirnov test and analyzed using a two-tailed Student's t-test when data are normally distributed. One sample t test and/or Wilcoxon test for unpaired samples was used when normally distributed population responses cannot be established. Differences between multiple groups were assessed by N-way analysis of variance (ANOVA) with the Tukey test or nonparametric Kruskal-Wallis test with the Dunn's test. The graphs were presented as mean ± Standard Deviation (SD).

Acknowledgments

We thank members of the Kim laboratory for their generous support. We appreciate thoughtful suggestion from Drs. Mike Tamkun, Sanghun Lee, and Bret Smith. This work is supported by Student Experiential Learning Grants from CSU, the NIH/NCATS Colorado CTSA Grant (UL1 TR002535), the Boettcher Foundation's Webb-Waring Biomedical Research Program, and the NIH grant (1R03AG072102).

References

1. G. B. D. Diseases, C. Injuries, Global burden of 369 diseases and injuries in 204 countries and territories, 1990-2019: a systematic analysis for the Global Burden of Disease Study 2019. *Lancet* **396**, 1204-1222 (2020).
2. E. J. Daly *et al.*, Health-related quality of life in depression: a STAR*D report. *Ann Clin Psychiatry* **22**, 43-55 (2010).
3. Z. Rihmer, X. Gonda, Prevention of depression-related suicides in primary care. *Psychiatr Hung* **27**, 72-81 (2012).
4. S. Moussavi *et al.*, Depression, chronic diseases, and decrements in health: results from the World Health Surveys. *Lancet* **370**, 851-858 (2007).
5. O. Berton, E. J. Nestler, New approaches to antidepressant drug discovery: beyond monoamines. *Nat Rev Neurosci* **7**, 137-151 (2006).
6. M. M. Katz *et al.*, Onset and early behavioral effects of pharmacologically different antidepressants and placebo in depression. *Neuropsychopharmacology : official publication of the American College of Neuropsychopharmacology* **29**, 566-579 (2004).
7. S. Kohtala, Ketamine-50 years in use: from anesthesia to rapid antidepressant effects and neurobiological mechanisms. *Pharmacol Rep* **73**, 323-345 (2021).
8. O. H. Miller, J. T. Moran, B. J. Hall, Two cellular hypotheses explaining the initiation of ketamine's antidepressant actions: Direct inhibition and disinhibition. *Neuropharmacology* **100**, 17-26 (2016).
9. C. G. Abdallah *et al.*, Ketamine's Mechanism of Action: A Path to Rapid-Acting Antidepressants. *Depress Anxiety* **33**, 689-697 (2016).
10. S. F. Grieco *et al.*, Psychedelics and Neural Plasticity: Therapeutic Implications. *J Neurosci* **42**, 8439-8449 (2022).

11. E. T. Kavalali, L. M. Monteggia, Targeting Homeostatic Synaptic Plasticity for Treatment of Mood Disorders. *Neuron* **106**, 715-726 (2020).

12. L. R. Aleksandrova, Y. T. Wang, A. G. Phillips, Ketamine and its metabolite, (2R,6R)-HNK, restore hippocampal LTP and long-term spatial memory in the Wistar-Kyoto rat model of depression. *Mol Brain* **13**, 92 (2020).

13. N. A. Anis, S. C. Berry, N. R. Burton, D. Lodge, The dissociative anaesthetics, ketamine and phencyclidine, selectively reduce excitation of central mammalian neurones by N-methyl-aspartate. *British journal of pharmacology* **79**, 565-575 (1983).

14. N. L. Harrison, M. A. Simmonds, Quantitative studies on some antagonists of N-methyl D-aspartate in slices of rat cerebral cortex. *British journal of pharmacology* **84**, 381-391 (1985).

15. M. M. Zarei, J. A. Dani, Ionic permeability characteristics of the N-methyl-D-aspartate receptor channel. *J Gen Physiol* **103**, 231-248 (1994).

16. A. Kawatake-Kuno, T. Murai, S. Uchida, A Multiscale View of the Mechanisms Underlying Ketamine's Antidepressant Effects: An Update on Neuronal Calcium Signaling. *Front Behav Neurosci* **15**, 749180 (2021).

17. F. Ali *et al.*, Ketamine disinhibits dendrites and enhances calcium signals in prefrontal dendritic spines. *Nat Commun* **11**, 72 (2020).

18. M. Lisek, L. Zylinska, T. Boczek, Ketamine and Calcium Signaling-A Crosstalk for Neuronal Physiology and Pathology. *Int J Mol Sci* **21** (2020).

19. G. H. Diering, R. L. Huganir, The AMPA Receptor Code of Synaptic Plasticity. *Neuron* **100**, 314-329 (2018).

20. H. K. Lee, Ca-permeable AMPA receptors in homeostatic synaptic plasticity. *Frontiers in molecular neuroscience* **5**, 17 (2012).

21. V. Duric *et al.*, Altered expression of synapse and glutamate related genes in post-mortem hippocampus of depressed subjects. *Int J Neuropsychopharmacol* **16**, 69-82 (2013).

22. S. Maeng *et al.*, Cellular mechanisms underlying the antidepressant effects of ketamine: role of alpha-amino-3-hydroxy-5-methylisoxazole-4-propionic acid receptors. *Biological psychiatry* **63**, 349-352 (2008).

23. H. Koike, S. Chaki, Requirement of AMPA receptor stimulation for the sustained antidepressant activity of ketamine and LY341495 during the forced swim test in rats. *Behavioural brain research* **271**, 111-115 (2014).

24. G. M. Chowdhury *et al.*, Transiently increased glutamate cycling in rat PFC is associated with rapid onset of antidepressant-like effects. *Molecular psychiatry* **22**, 120-126 (2017).

25. B. Moghaddam, B. Adams, A. Verma, D. Daly, Activation of glutamatergic neurotransmission by ketamine: a novel step in the pathway from NMDA receptor blockade to dopaminergic and cognitive disruptions associated with the prefrontal cortex. *J Neurosci* **17**, 2921-2927 (1997).

26. K. S. El Iskandrani, C. A. Oosterhof, M. El Mansari, P. Blier, Impact of subanesthetic doses of ketamine on AMPA-mediated responses in rats: An in vivo electrophysiological study on monoaminergic and glutamatergic neurons. *J Psychopharmacol* **29**, 792-801 (2015).

27. E. Nosyreva *et al.*, Acute suppression of spontaneous neurotransmission drives synaptic potentiation. *J Neurosci* **33**, 6990-7002 (2013).

28. P. Zanos *et al.*, NMDAR inhibition-independent antidepressant actions of ketamine metabolites. *Nature* **533**, 481-486 (2016).

29. B. Yang *et al.*, Comparison of R-ketamine and rapastinel antidepressant effects in the social defeat stress model of depression. *Psychopharmacology* **233**, 3647-3657 (2016).

30. N. Li *et al.*, mTOR-dependent synapse formation underlies the rapid antidepressant effects of NMDA antagonists. *Science* **329**, 959-964 (2010).

31. P. Georgiou *et al.*, Experimenters' sex modulates mouse behaviors and neural responses to ketamine via corticotropin releasing factor. *Nat Neurosci* **25**, 1191-1200 (2022).

32. J. T. Isaac, M. C. Ashby, C. J. McBain, The role of the GluR2 subunit in AMPA receptor function and synaptic plasticity. *Neuron* **54**, 859-871 (2007).

33. S. J. Liu, R. S. Zukin, Ca2+-permeable AMPA receptors in synaptic plasticity and neuronal death. *Trends Neurosci* **30**, 126-134 (2007).

34. M. F. Sathler *et al.*, Phosphorylation of the AMPA receptor subunit GluA1 regulates clathrin-mediated receptor internalization. *Journal of cell science* **134** (2021).

35. S. Kim, E. B. Ziff, Calcineurin mediates synaptic scaling via synaptic trafficking of Ca2+-permeable AMPA receptors. *PLoS biology* **12**, e1001900 (2014).

36. O. Skiteva, N. Yao, K. Chergui, Ketamine induces opposite changes in AMPA receptor calcium permeability in the ventral tegmental area and nucleus accumbens. *Transl Psychiatry* **11**, 530 (2021).

37. P. Hartvig *et al.*, Central nervous system effects of subdissociative doses of (S)-ketamine are related to plasma and brain concentrations measured with positron emission tomography in healthy volunteers. *Clin Pharmacol Ther* **58**, 165-173 (1995).

38. S. Kim *et al.*, Network compensation of cyclic GMP-dependent protein kinase II knockout in the hippocampus by Ca2+-permeable AMPA receptors. *Proc Natl Acad Sci U S A* **112**, 3122-3127 (2015).

39. S. Kim, C. J. Violette, E. B. Ziff, Reduction of increased calcineurin activity rescues impaired homeostatic synaptic plasticity in presenilin 1 M146V mutant. *Neurobiol Aging* **36**, 3239-3246 (2015).

40. J. P. Roberts, S. A. Stokoe, M. F. Sathler, R. A. Nichols, S. Kim, Selective co-activation of alpha7- and alpha4beta2-nicotinic acetylcholine receptors reverses beta-amyloid-induced synaptic dysfunction. *The Journal of biological chemistry* 10.1016/j.jbc.2021.100402, 100402 (2021).

41. J. L. Sun *et al.*, Co-activation of selective nicotinic acetylcholine receptors is required to reverse beta amyloid-induced Ca(2+) hyperexcitation. *Neurobiol Aging* **84**, 166-177 (2019).

42. K. Sztukowski *et al.*, HIV induces synaptic hyperexcitation via cGMP-dependent protein kinase II activation in the FIV infection model. *PLoS biology* **16**, e2005315 (2018).

43. K. Zhang *et al.*, Essential roles of AMPA receptor GluA1 phosphorylation and presynaptic HCN channels in fast-acting antidepressant responses of ketamine. *Science signaling* **9**, ra123 (2016).

44. M. Asim, B. Hao, A. Waris, Y. M. Liang, X. G. Wang, Ketamine attenuates the PTSD-like effect via regulation of glutamatergic signaling in the nucleus accumbens of mice. *Mol Cell Neurosci* **120**, 103723 (2022).

45. K. Zhang, V. N. Yamaki, Z. Wei, Y. Zheng, X. Cai, Differential regulation of GluA1 expression by ketamine and memantine. *Behavioural brain research* **316**, 152-159 (2017).

46. B. D. Hare *et al.*, Optogenetic stimulation of medial prefrontal cortex Drd1 neurons produces rapid and long-lasting antidepressant effects. *Nat Commun* **10**, 223 (2019).

47. R. F. Halliwell, J. A. Peters, J. J. Lambert, The mechanism of action and pharmacological specificity of the anticonvulsant NMDA antagonist MK-801: a voltage clamp study on neuronal cells in culture. *British journal of pharmacology* **96**, 480-494 (1989).

48. H. Dana *et al.*, High-performance calcium sensors for imaging activity in neuronal populations and microcompartments. *Nature methods* **16**, 649-657 (2019).

49. S. Mehta, J. Zhang, Using a genetically encoded FRET-based reporter to visualize calcineurin phosphatase activity in living cells. *Methods in molecular biology* **1071**, 139-149 (2014).

50. P. Osten *et al.*, Mutagenesis reveals a role for ABP/GRIP binding to GluR2 in synaptic surface accumulation of the AMPA receptor. *Neuron* **27**, 313-325 (2000).

51. J. Liu *et al.*, Calcineurin is a common target of cyclophilin-cyclosporin A and FKBP-FK506 complexes. *Cell* **66**, 807-815 (1991).

52. M. Gleichmann, M. P. Mattson, Neuronal calcium homeostasis and dysregulation. *Antioxid Redox Signal* **14**, 1261-1273 (2011).

53. Y. Yang, W. Ju, H. Zhang, L. Sun, Effect of Ketamine on LTP and NMDAR EPSC in Hippocampus of the Chronic Social Defeat Stress Mice Model of Depression. *Front Behav Neurosci* **12**, 229 (2018).

54. Z. Jia *et al.*, Enhanced LTP in mice deficient in the AMPA receptor GluR2. *Neuron* **17**, 945-956 (1996).

55. M. Farooq *et al.*, Lithium increases synaptic GluA2 in hippocampal neurons by elevating the delta-catenin protein. *Neuropharmacology* 10.1016/j.neuropharm.2016.10.025 (2016).

56. S. Kim, J. Shou, S. Abera, E. B. Ziff, Sucrose withdrawal induces depression and anxiety-like behavior by Kir2.1 upregulation in the nucleus accumbens. *Neuropharmacology* **130**, 10-17 (2018).

57. J. Shou, A. Tran, N. Snyder, E. Bleem, S. Kim, Distinct Roles of GluA2-lacking AMPA Receptor Expression in Dopamine D1 or D2 Receptor Neurons in Animal Behavior. *Neuroscience* **398**, 102-112 (2018).

58. M. Chatterjee, S. Ganguly, M. Srivastava, G. Palit, Effect of 'chronic' versus 'acute' ketamine administration and its 'withdrawal' effect on behavioural alterations in mice: implications for experimental psychosis. *Behavioural brain research* **216**, 247-254 (2011).

59. K. Akillioglu, E. B. Melik, E. Melik, A. Boga, Effect of ketamine on exploratory behaviour in BALB/C and C57BL/6 mice. *Pharmacol Biochem Behav* **100**, 513-517 (2012).

60. F. Y. de Araujo *et al.*, Inhibition of ketamine-induced hyperlocomotion in mice by the essential oil of Alpinia zerumbet: possible involvement of an antioxidant effect. *J Pharm Pharmacol* **63**, 1103-1110 (2011).

61. M. Irifune, T. Shimizu, M. Nomoto, Ketamine-induced hyperlocomotion associated with alteration of presynaptic components of dopamine neurons in the nucleus accumbens of mice. *Pharmacol Biochem Behav* **40**, 399-407 (1991).

62. B. E. Hetzler, B. S. Wautlet, Ketamine-induced locomotion in rats in an open-field. *Pharmacol Biochem Behav* **22**, 653-655 (1985).

63. F. Razoux, R. Garcia, I. Lena, Ketamine, at a dose that disrupts motor behavior and latent inhibition, enhances prefrontal cortex synaptic efficacy and glutamate release in the nucleus accumbens. *Neuropsychopharmacology : official publication of the American College of Neuropsychopharmacology* **32**, 719-727 (2007).

64. N. Adotevi *et al.*, alpha-Amino-3-Hydroxy-5-Methyl-4-Isoxazolepropionic Acid Receptor Plasticity Sustains Severe, Fatal Status Epilepticus. *Ann Neurol* **87**, 84-96 (2020).

65. E. Szczurowska, P. Mares, An antagonist of calcium permeable AMPA receptors, IEM1460: Anticonvulsant action in immature rats? *Epilepsy Res* **109**, 106-113 (2015).

66. T. C. Thiagarajan, M. Lindskog, R. W. Tsien, Adaptation to synaptic inactivity in hippocampal neurons. *Neuron* **47**, 725-737 (2005).

67. S. D. Sun *et al.*, Synaptic homeostasis transiently leverages Hebbian mechanisms for a multiphasic response to inactivity. *bioRxiv* 10.1101/2022.06.18.496642, 2022.2006.2018.496642 (2022).

68. I. H. Greger, J. F. Watson, S. G. Cull-Candy, Structural and Functional Architecture of AMPA-Type Glutamate Receptors and Their Auxiliary Proteins. *Neuron* **94**, 713-730 (2017).

69. J. E. Pick, E. B. Ziff, Regulation of AMPA receptor trafficking and exit from the endoplasmic reticulum. *Mol Cell Neurosci* **91**, 3-9 (2018).

70. V. A. Derkach, M. C. Oh, E. S. Guire, T. R. Soderling, Regulatory mechanisms of AMPA receptors in synaptic plasticity. *Nat Rev Neurosci* **8**, 101-113 (2007).

71. Y. Serulle *et al.*, A GluR1-cGKII interaction regulates AMPA receptor trafficking. *Neuron* **56**, 670-688 (2007).

72. K. W. Roche, R. J. O'Brien, A. L. Mammen, J. Bernhardt, R. L. Huganir, Characterization of multiple phosphorylation sites on the AMPA receptor GluR1 subunit. *Neuron* **16**, 1179-1188 (1996).

73. T. G. Banke *et al.*, Control of GluR1 AMPA receptor function by cAMP-dependent protein kinase. *J Neurosci* **20**, 89-102 (2000).

74. M. D. Ehlers, Reinsertion or degradation of AMPA receptors determined by activity-dependent endocytic sorting. *Neuron* **28**, 511-525 (2000).

75. J. A. Esteban *et al.*, PKA phosphorylation of AMPA receptor subunits controls synaptic trafficking underlying plasticity. *Nat Neurosci* **6**, 136-143 (2003).

76. H. K. Lee *et al.*, Phosphorylation of the AMPA receptor GluR1 subunit is required for synaptic plasticity and retention of spatial memory. *Cell* **112**, 631-643 (2003).

77. M. C. Oh, V. A. Derkach, E. S. Guire, T. R. Soderling, Extrasynaptic membrane trafficking regulated by GluR1 serine 845 phosphorylation primes AMPA receptors for long-term potentiation. *The Journal of biological chemistry* **281**, 752-758 (2006).

78. H. Y. Man, Y. Sekine-Aizawa, R. L. Huganir, Regulation of {alpha}-amino-3-hydroxy-5-methyl-4-isoxazolepropionic acid receptor trafficking through PKA phosphorylation of the Glu receptor 1 subunit. *Proc Natl Acad Sci U S A* **104**, 3579-3584 (2007).

79. G. H. Diering, A. S. Gustina, R. L. Huganir, PKA-GluA1 coupling via AKAP5 controls AMPA receptor phosphorylation and cell-surface targeting during bidirectional homeostatic plasticity. *Neuron* **84**, 790-805 (2014).

80. H. K. Lee, M. Barbarosie, K. Kameyama, M. F. Bear, R. L. Huganir, Regulation of distinct AMPA receptor phosphorylation sites during bidirectional synaptic plasticity. *Nature* **405**, 955-959 (2000).

81. V. Derkach, A. Barria, T. R. Soderling, Ca2+/calmodulin-kinase II enhances channel conductance of alpha-amino-3-hydroxy-5-methyl-4-isoxazolepropionate type glutamate receptors. *Proc Natl Acad Sci U S A* **96**, 3269-3274 (1999).

82. A. S. Kristensen *et al.*, Mechanism of Ca2+/calmodulin-dependent kinase II regulation of AMPA receptor gating. *Nat Neurosci* **14**, 727-735 (2011).

83. A. Barria, D. Muller, V. Derkach, L. C. Griffith, T. R. Soderling, Regulatory phosphorylation of AMPA-type glutamate receptors by CaM-KII during long-term potentiation. *Science* **276**, 2042-2045 (1997).

84. P. Park *et al.*, The Role of Calcium-Permeable AMPARs in Long-Term Potentiation at Principal Neurons in the Rodent Hippocampus. *Front Synaptic Neurosci* **10**, 42 (2018).

85. K. M. Noh *et al.*, Blockade of calcium-permeable AMPA receptors protects hippocampal neurons against global ischemia-induced death. *Proc Natl Acad Sci U S A* **102**, 12230-12235 (2005).

86. R. B. Dias, D. M. Rombo, J. A. Ribeiro, A. M. Sebastiao, Ischemia-induced synaptic plasticity drives sustained expression of calcium-permeable AMPA receptors in the hippocampus. *Neuropharmacology* **65**, 114-122 (2013).

87. A. Wojtas *et al.*, Effect of Psilocybin and Ketamine on Brain Neurotransmitters, Glutamate Receptors, DNA and Rat Behavior. *Int J Mol Sci* **23** (2022).

88. N. Yao, O. Skiteva, X. Zhang, P. Svenningsson, K. Chergui, Ketamine and its metabolite (2R,6R)-hydroxynorketamine induce lasting alterations in glutamatergic synaptic plasticity in the mesolimbic circuit. *Molecular psychiatry* **23**, 2066-2077 (2018).

89. A. Franceschelli, J. Sens, S. Herchick, C. Thelen, P. M. Pitychoutis, Sex differences in the rapid and the sustained antidepressant-like effects of ketamine

in stress-naive and "depressed" mice exposed to chronic mild stress. *Neuroscience* **290**, 49-60 (2015).

90. N. Carrier, M. Kabbaj, Sex differences in the antidepressant-like effects of ketamine. *Neuropharmacology* **70**, 27-34 (2013).

91. A. M. Dossat, K. N. Wright, C. E. Strong, M. Kabbaj, Behavioral and biochemical sensitivity to low doses of ketamine: Influence of estrous cycle in C57BL/6 mice. *Neuropharmacology* **130**, 30-41 (2018).

92. S. K. Saland, M. Kabbaj, Sex Differences in the Pharmacokinetics of Low-dose Ketamine in Plasma and Brain of Male and Female Rats. *J Pharmacol Exp Ther* **367**, 393-404 (2018).

93. S. K. Saland, K. J. Schoepfer, M. Kabbaj, Hedonic sensitivity to low-dose ketamine is modulated by gonadal hormones in a sex-dependent manner. *Sci Rep* **6**, 21322 (2016).

94. M. F. Ho *et al.*, Ketamine and ketamine metabolites as novel estrogen receptor ligands: Induction of cytochrome P450 and AMPA glutamate receptor gene expression. *Biochemical pharmacology* **152**, 279-292 (2018).

95. J. A. Avila *et al.*, Estradiol rapidly increases GluA2-mushroom spines and decreases GluA2-filopodia spines in hippocampus CA1. *Hippocampus* **27**, 1224-1229 (2017).

96. J. Wei *et al.*, Estrogen protects against the detrimental effects of repeated stress on glutamatergic transmission and cognition. *Molecular psychiatry* **19**, 588-598 (2014).

97. C. Holden, Sex and the suffering brain. *Science* **308**, 1574 (2005).

98. R. C. Kessler *et al.*, Prevalence and treatment of mental disorders, 1990 to 2003. *N Engl J Med* **352**, 2515-2523 (2005).

99. M. Steiner *et al.*, Gender differences in clinical presentation and response to sertraline treatment of generalized anxiety disorder. *Hum Psychopharmacol* **20**, 3-13 (2005).

100. R. C. Kessler *et al.*, The epidemiology of major depressive disorder: results from the National Comorbidity Survey Replication (NCS-R). *JAMA* **289**, 3095-3105 (2003).

101. M. P. Cosgrove, L. A. Sargeant, S. J. Griffin, Does depression increase the risk of developing type 2 diabetes? *Occup Med (Lond)* **58**, 7-14 (2008).

102. G. M. Hosang, C. Shiles, K. E. Tansey, P. McGuffin, R. Uher, Interaction between stress and the BDNF Val66Met polymorphism in depression: a systematic review and meta-analysis. *BMC Med* **12**, 7 (2014).

103. J. P. Bonde *et al.*, Risk of depressive disorder following disasters and military deployment: systematic review with meta-analysis. *Br J Psychiatry* **208**, 330-336 (2016).

104. R. G. Weston, P. J. Fitzgerald, B. O. Watson, Repeated Dosing of Ketamine in the Forced Swim Test: Are Multiple Shots Better Than One? *Frontiers in psychiatry* **12**, 659052 (2021).

105. X. C. Ma *et al.*, Long-lasting antidepressant action of ketamine, but not glycogen synthase kinase-3 inhibitor SB216763, in the chronic mild stress model of mice. *PLoS One* **8**, e56053 (2013).

106. C. Dong *et al.*, Rapid and Sustained Antidepressant Action of the mGlu2/3 Receptor Antagonist MGS0039 in the Social Defeat Stress Model: Comparison with Ketamine. *Int J Neuropsychopharmacol* **20**, 228-236 (2017).

107. W. J. Zhang *et al.*, Downregulation of Egr-1 Expression Level via GluN2B Underlies the Antidepressant Effects of Ketamine in a Chronic Unpredictable Stress Animal Model of Depression. *Neuroscience* **372**, 38-45 (2018).

108. C. A. Browne, E. Falcon, S. A. Robinson, O. Berton, I. Lucki, Reversal of Stress-Induced Social Interaction Deficits by Buprenorphine. *Int J Neuropsychopharmacol* **21**, 164-174 (2018).

109. A. C. Nugent *et al.*, Ketamine has distinct electrophysiological and behavioral effects in depressed and healthy subjects. *Molecular psychiatry* **24**, 1040-1052 (2019).

110. D. M. Gerhard *et al.*, GABA interneurons are the cellular trigger for ketamine's rapid antidepressant actions. *J Clin Invest* **130**, 1336-1349 (2020).

111. P. Zanos, S. M. Thompson, R. S. Duman, C. A. Zarate, Jr., T. D. Gould, Convergent Mechanisms Underlying Rapid Antidepressant Action. *CNS Drugs* **32**, 197-227 (2018).

112. D. J. Newport *et al.*, Ketamine and Other NMDA Antagonists: Early Clinical Trials and Possible Mechanisms in Depression. *Am J Psychiatry* **172**, 950-966 (2015).

113. M. F. Sathler *et al.*, HIV and FIV glycoproteins increase cellular tau pathology via cGMP-dependent kinase II activation. *Journal of cell science* **135** (2022).

114. B. J. Wiltgen *et al.*, A role for calcium-permeable AMPA receptors in synaptic plasticity and learning. *PLoS One* **5** (2010).

115. S. Kim, A. N. Lapham, C. G. Freedman, T. L. Reed, W. K. Schmidt, Yeast as a tractable genetic system for functional studies of the insulin-degrading enzyme. *The Journal of biological chemistry* **280**, 27481-27490 (2005).

116. S. Kim *et al.*, Brain region-specific effects of cGMP-dependent kinase II knockout on AMPA receptor trafficking and animal behavior. *Learning & memory* **23**, 435-441 (2016).

117. S. Kim *et al.*, Evidence that the rab5 effector APPL1 mediates APP-betaCTF-induced dysfunction of endosomes in Down syndrome and Alzheimer's disease. *Molecular psychiatry* 10.1038/mp.2015.97 (2015).

118. T. M. Tran *et al.*, Loss of cGMP-dependent protein kinase II alters ultrasonic vocalizations in mice, a model for speech impairment in human microdeletion 4q21 syndrome. *Neuroscience letters* **759**, 136048 (2021).

119. J. Y. Kim *et al.*, Viral transduction of the neonatal brain delivers controllable genetic mosaicism for visualising and manipulating neuronal circuits in vivo. *The European journal of neuroscience* **37**, 1203-1220 (2013).

120. A. R. Wild *et al.*, Synapse-to-Nucleus Communication through NFAT Is Mediated by L-type Ca(2+) Channel Ca(2+) Spike Propagation to the Soma. *Cell Rep* **26**, 3537-3550 e3534 (2019).

121. T. Furuta *et al.*, In vivo transduction of central neurons using recombinant Sindbis virus: Golgi-like labeling of dendrites and axons with membrane-targeted fluorescent proteins. *J Histochem Cytochem* **49**, 1497-1508 (2001).

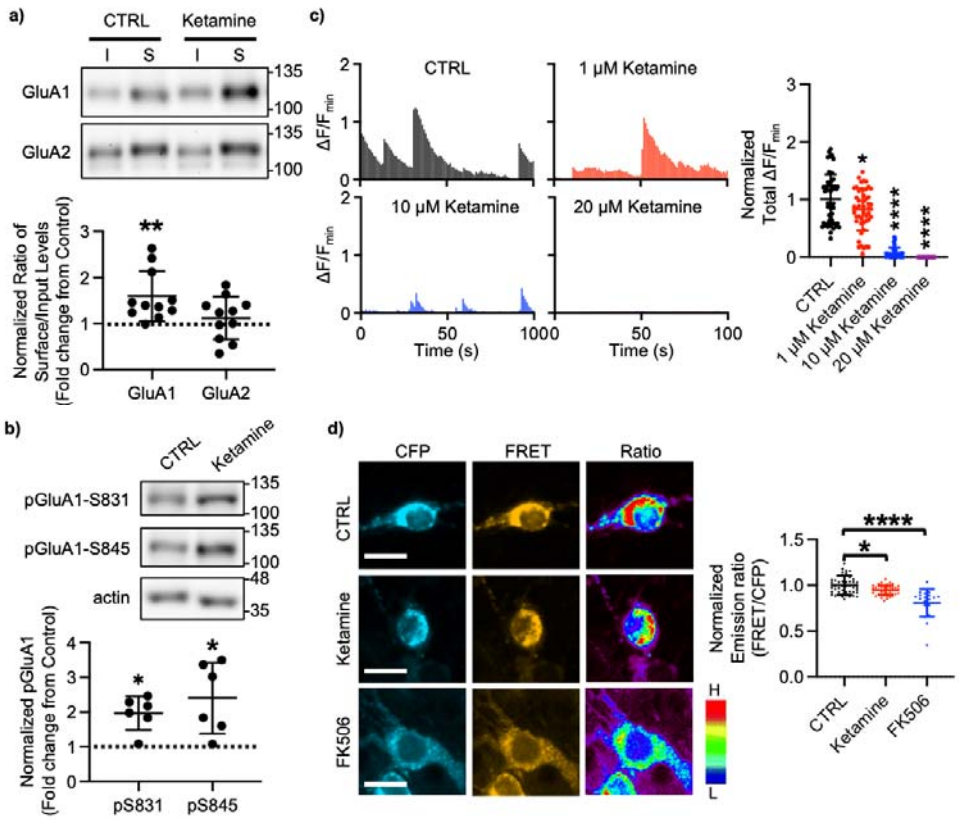

Figure 1. Ketamine treatment selectively increases GluA1-containing AMPAR surface expression by decreasing calcineurin activity in cultured mouse hippocampal neurons. **a)** Representative immunoblots of input (I) and surface (S) levels in control (CTRL) and ketamine-treated neurons. Summary bar graphs of normalized surface GluA1 and GluA2 levels in each condition (n = 11 immunoblots from 4 independent cultures, $^{**}p < 0.01$, One sample t and Wilcoxon test). **b)** Representative immunoblots of pGluA1 levels in control (CTRL) and ketamine-treated neurons. Summary graphs of normalized GluA1 phosphorylation levels in each condition (n = 6 immunoblots from 3 independent cultures, $^{*}p < 0.05$, One sample t and Wilcoxon test). **c)** Representative traces of GCaMP7s signals in excitatory cells and summary data of normalized total Ca^{2+} activity in each condition (n = number of neurons from 2 independent cultures, CTRL = 46, 1 μM Ketamine = 49, 10 μM Ketamine = 27, and 20 μM Ketamine = 19, $^{*}p < 0.05$ and $^{****}p < 0.0001$, One-way ANOVA with the Tukey test). **d)** Representative images of a CFP channel, a FRET channel, and a pseudocolored emission ratio (Y/C) in each condition [blue (L), low emission ratio; red (H), high emission ratio]. Scale bar is 10 μm. A summary graph showing average of emission ratio (Y/C) in each condition (n = number of cells, CTRL = 47, ketamine = 44, and FK506 = 20 from 2 independent cultures; $^{*}p < 0.05$ and $^{****}p < 0.0001$; One-way ANOVA with the Tukey test). A scale bar indicates 10 μm.

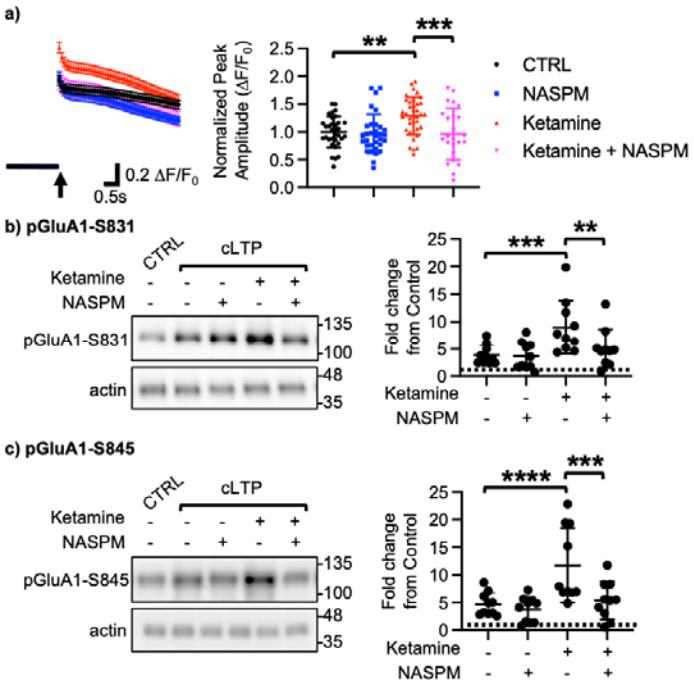

Figure 2. Ketamine treatment induces CP-AMPAR expression to enhance glutamatergic activity and synaptic plasticity in cultured mouse hippocampal neurons. a) Average traces of virally expressed GCaMP7s signals, and summary data of normalized peak amplitude in each condition (n = number of neurons, CTRL = 33, NASPM = 32, Ketamine = 37, and Ketamine + NASPM = 24 from 2 independent cultures; $^{**}p < 0.01$ and $^{***}p < 0.001$; Two-way ANOVA with the Tukey test). An arrow indicates photostimulation. Representative immunoblots and quantitative analysis of **b)** pGluA1-S831 and **c)** pGluA1-S845 levels in each condition (n = 10 immunoblots from 5 independent cultures, $^{**}p < 0.01$, $^{***}p < 0.001$, and $^{****}p < 0.0001$, the Kruskal-Wallis test with the Dunn's test).

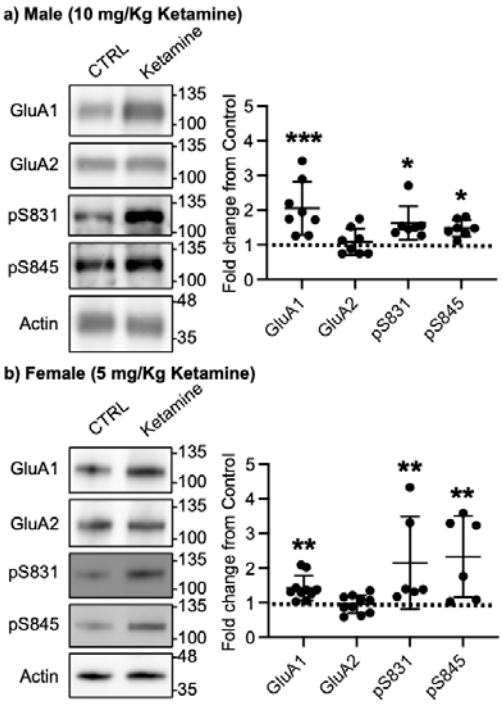

Figure 3. Synaptic GluA1 levels are selectively increased in the hippocampus following ketamine treatment. Representative immunoblots of AMPAR levels in the hippocampus of control (CTRL) and ketamine-treated **a)** males and **b)** females. Summary graphs of normalized GluA1, GluA2, and GluA1 phosphorylation levels in each condition (n = number of immunoblots from 4 male and 3 female mice in each condition; Male, CTRL = 8, GluA1 = 8, GluA2 = 8, pS831 = 7, and pS845 = 7, Female, CTRL = 10, GluA1 = 10, GluA2 = 10, pS831 = 6, and pS845 = 6, *$p < 0.05$ and **$p < 0.01$; One sample t and Wilcoxon test).

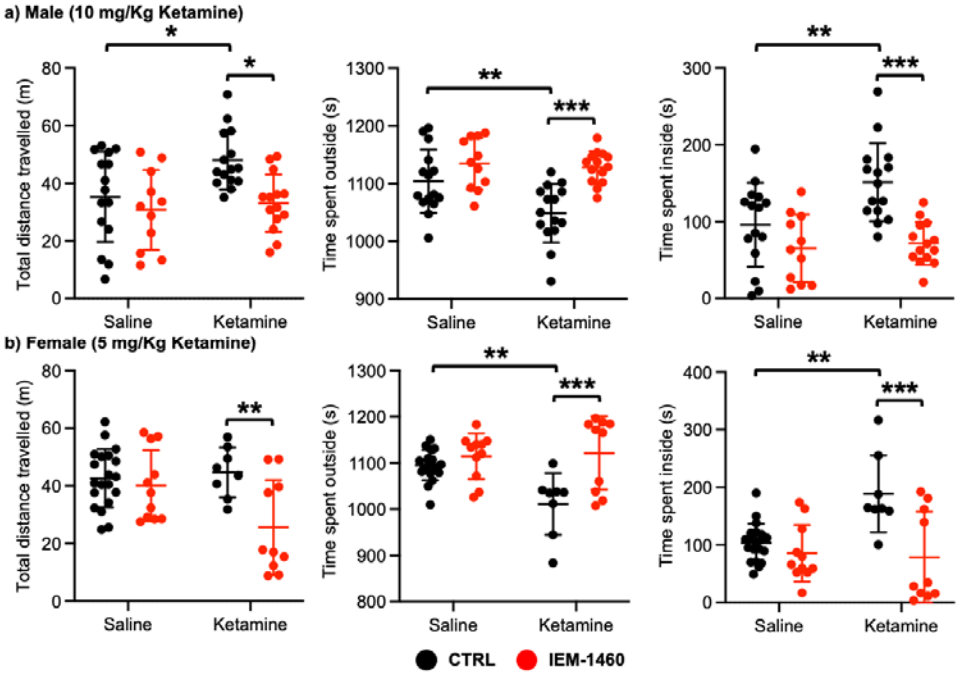

Figure 4. Ketamine treatment significantly reduces anxiety-like behavior in mice, which requires CP-AMPARs. The results of the open field test measuring total distance travelled and time spent outside and inside in **a)** male and **b)** female mice in each condition (n = number of mice, Male; saline = 15, IEM 1460 = 11, Ketamine = 15, and Ketamine + IEM 1460 = 14, Female; saline = 20, IEM 1460 = 11, Ketamine = 8, and Ketamine + IEM 1460 = 10, *$p < 0.05$, **$p < 0.01$, and ***$p < 0.001$, Two-way ANOVA with the Tukey test).

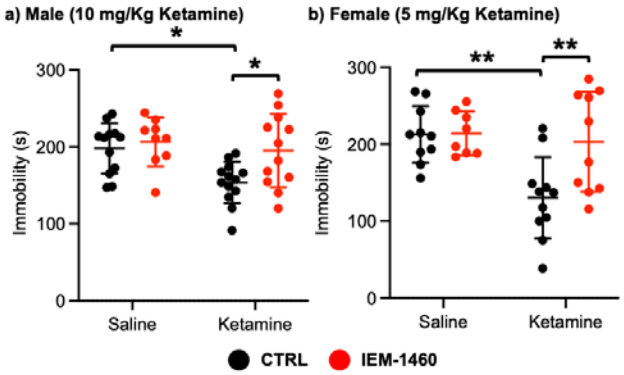

Figure 5. Ketamine treatment significantly reduces depression-like behavior in mice, which requires CP-AMPARs. The results of the tail suspension test measuring total immobility in **a)** male and **b)** female mice in each condition (n = number of mice, Male; saline = 12, IEM 1460 = 9, Ketamine = 13, and Ketamine + IEM 1460 = 12, Female; saline = 10, IEM 1460 = 8, Ketamine = 11, and Ketamine + IEM 1460 = 10, *$p < 0.05$ and **$p < 0.01$, Two-way ANOVA with the Tukey test).

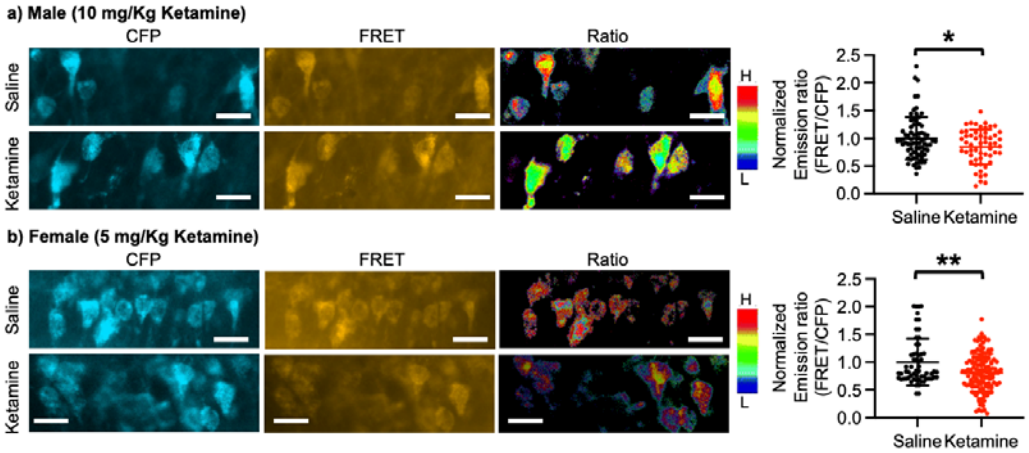

Figure 6. Ketamine treatment significantly reduces calcineurin activity in the hippocampus. Representative images of a CFP channel, a FRET channel, and a pseudocolored emission ratio (Y/C) in the **a)** male and **b)** female hippocampus in each condition [blue (L), low emission ratio; red (H), high emission ratio]. Scale bar is 10 µm. A summary graph showing average of emission ratio (FRET/CFP) in each condition (n = number of cells [number of animals], Male; saline = 74 [7] and ketamine = 55 [5], Female; saline = 61 [7] and ketamine = 130 [4], *$p < 0.05$ and **$p < 0.01$, unpaired two-tailed student t-test). A scale bar indicates 25 µm.

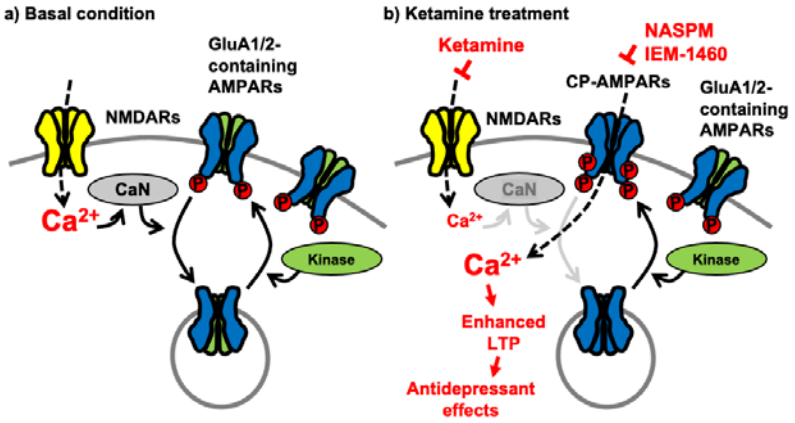

Figure 7. A schematic model of ketamine's antidepressant effects. a) Under the basal conditions, stimulation of excitatory synapses results in Ca^{2+} influx through glutamatergic NMDA receptors (NMDARs), which initiates intracellular pathways for synaptic plasticity. NMDAR-mediated Ca^{2+} can activate calcineurin (CaN), a Ca^{2+}-dependent phosphatase that dephosphorylates the AMPA receptor (AMPAR) subunit GluA1, leading to AMPAR endocytosis. Several kinases, including PKA, cGKII, PKC, and CaMKII, on the other hand, can phosphorylate GluA1 to promote AMPAR surface expression. As a result, AMPAR trafficking and synaptic activity are controlled by the balance of kinases and phosphatases. **b)** Because ketamine is a noncompetitive NMDAR antagonist, a therapeutic dose is enough to block NMDAR-mediated Ca^{2+} influx in excitatory synapses. This can lower CaN activation and promote GluA1 phosphorylation, resulting in increased synaptic expression of GluA2-lacking, GluA1-containing Ca^{2+}-permeable AMPARs (CP-AMPARs). When ketamine is administered, CP-AMPAR-mediated Ca^{2+} influx may replace NMDA-dependent Ca^{2+} signaling. This increases synaptic plasticity, which leads to antidepressant benefits from ketamine.

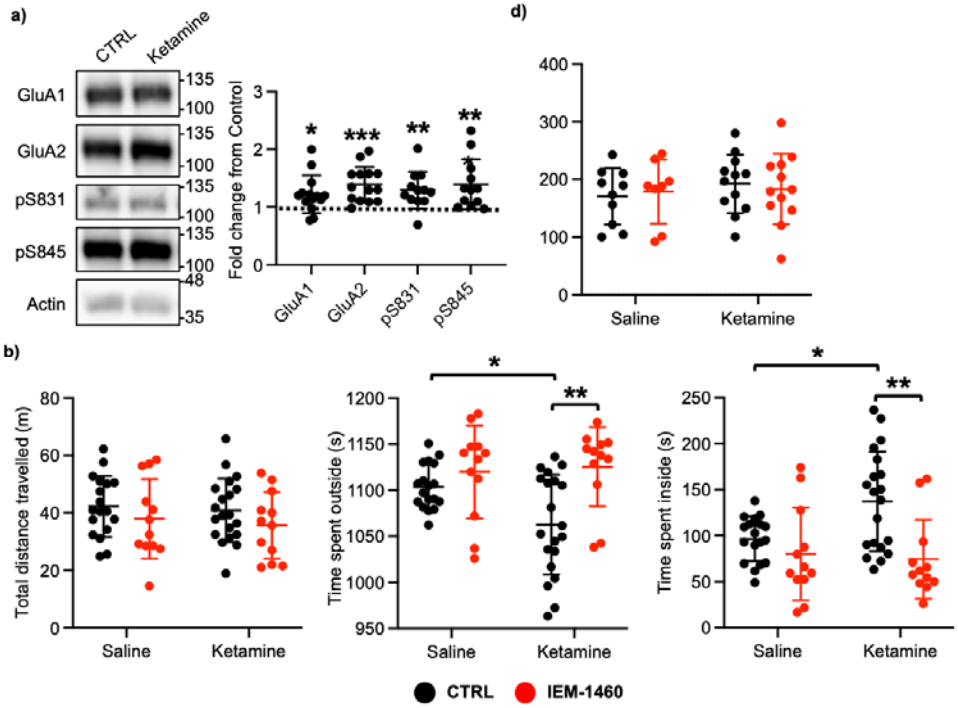

Supplementary Figure 1. The effects of 10 mg/kg ketamine treatment in female mice. a) Representative immunoblots of AMPAR levels in the hippocampus of control (CTRL) and 10mg/kg ketamine-treated female mice. Summary graphs of normalized GluA1, GluA2, and GluA1 phosphorylation levels in each condition (n = number of immunoblots from 4 female mice in each condition; CTRL = 14, GluA1 = 14, GluA2 = 14, pS831 = 12, and pS845 = 12, *$p < 0.05$, **$p < 0.01$, and ***$p < 0.001$; One sample t and Wilcoxon test). **b)** The results of the open field test measuring total distance travelled and time spent outside and inside in female mice in each condition (n = number of mice, saline = 18, IEM 1460 = 12, Ketamine = 20, and Ketamine + IEM 1460 = 17, *$p < 0.05$ and **$p < 0.01$, Two-way ANOVA with the Tukey test). **c)** The results of the tail suspension test measuring total immobility in female mice in each condition (n = number of mice, saline = 10, IEM 1460 = 8, Ketamine = 12, and Ketamine + IEM 1460 = 12, Two-way ANOVA with the Tukey test).